Transmembrane Domain Analysis of Polycystin-1, the Product of the Polycystic Kidney Disease-1 (PKD1) Gene: Evidence for 11 Membrane-Spanning Domains†

Nancy Nims, Dianne Vassmer, and Robin L. Maser*

Department of Biochemistry and Molecular Biology, University of Kansas Medical Center, Kansas City, Kansas 66160-7421

Received June 23, 2003; Revised Manuscript Received September 14, 2003

ABSTRACT: Polycystin-1, the protein product of the polycystic kidney disease-1 (PKD1) gene, was originally predicted to be an integral membrane glycoprotein with 11 transmembrane (TM) domains (TM 1−11). Subsequent comparative sequence analyses led to a revision of the original model, which retained the overall topology and 11 TM segments (TM I−XI) but dropped 3 of the original domains and introduced 3 new TM domains. The membrane-spanning potential and the orientation of each of the proposed TM domains following the extracellular REJ domain (TM I−XI and TM 11) have now been tested. Using a series of N-terminal polycystin TM-glycosylation reporter gene fusions expressed in vivo, we assayed N-linked glycosylation of the C-terminal glycosylation reporter as an indicator of TM domain presence and orientation. This approach has clearly demonstrated that 7 of the 12 TM domains tested function as membrane-spanning domains. In vitro analysis of the topogenic potential of the five remaining TM domains revealed that four of these also function as membrane-spanning domains, thus supporting an 11 TM structure for polycystin-1 comprised of TM domains I−XI. In addition, these studies suggest that the membrane insertion of TM domains I−IX occurs in a cotranslational and sequential manner, while multiple topogenic determinants appear to be required for the integration of the C-terminal-most TM segments of polycystin-1.

Autosomal dominant polycystic kidney disease (ADPKD)[1] is a common genetic disease affecting one in every thousand individuals and accounting for up to 10% of kidney replacement health care costs (reviewed in ref *1*). The primary characteristic of PKD is the development and expansion of hundreds of fluid-filled cysts that arise from the tubules of affected kidneys. The majority of ADPKD cases result from mutations within the PKD1 gene which encodes a large (4302 residue), integral membrane glycoprotein, polycystin-1 (*2*). Polycystin-1 is thought to be part of a plasma membrane signaling/ion channel complex involved in maintaining the terminally differentiated state of renal tubular epithelial cells (*3*, *4*). Initial sequence analyses of human polycystin-1 resulted in a structural model consisting of an ∼2500 amino acid extracellular N-terminal portion followed by 11 membrane-spanning or transmembrane (TM) domains (TM 1−11) and a 226 amino acid, intracellular C-terminal tail (*5*). Later comparative analyses of polycystin-1 with human polycystin-2 (*6*), Fugu polycystin-1 (*7*), and sea urchin receptor for egg jelly (REJ) (*8*) protein sequences led to a revision of the original model which retained the overall topology and 11 TM segments (TM I−XI) but dropped 3 of the original domains and introduced 3 new TM domains (*7*). These changes resulted in an increase in the length of the N-terminal extracellular domain and a decrease in the length of the cytosolic, C-terminal tail.

Although polycystin-1 has been demonstrated to be a glycosylated integral membrane protein with N-terminal extracellular binding and C-terminal intracellular signal transduction properties (*9*−*14*), there are no biochemical studies that address the validity of the proposed membrane-spanning domains. Furthermore, polycystin-1 has been shown to bind and activate heterotrimeric G proteins (*15*−*17*) and to be cleaved at its proposed heterotrimeric G protein-coupled receptor proteolytic cleavage site (GPS) (*18*), a feature common to members of the long N-terminal family B (LNB-TM7) of heterotrimeric G protein-coupled receptors (GPCRs) (*19*−*21*). These observations suggest that polycystin-1 could have an alternate structure, perhaps resembling the classical 7 TM heterotrimeric GPCRs (*22*).

Polytopic membrane proteins are synthesized at the rough endoplasmic reticulum (ER) where they are cotranslationally integrated within the ER membrane through a multiprotein pore complex, the translocon, to achieve their final topology (*23*). The membrane topology of a polypeptide is determined by topogenic information encoded within nascent TM domains and associated loop sequences (*24*). The topogenic signals for polytopic membrane proteins are thought to exist as alternating start and stop transfer (or translocation) sequences. Sequences which direct translocation of their N-terminus to achieve an $N_{exo}-C_{cyto}$ orientation are termed type I signal anchors, while those that direct translocation

† This work was supported by grants from the PKD Foundation (98011) and the NIH/NIDDK (P50-DK57301).

* To whom correspondence should be addressed. Tel: 913-588-7425. Fax: 913-588-7440. E-mail: rmaser@kumc.edu.

[1] Abbreviations: aa, amino acid; ActD, actinomycin D; ADPKD, autosomal dominant polycystic kidney disease; CX, cycloheximide; GPCR, G protein-coupled receptor; GPS, GPCR proteolytic cleavage site; HA, hemagglutinin; N3, three consensus N-linked glycosylation sites; N-gF, *N*-glycosidase F; PRL, prolactin; ProK, proteinase K; REJ, receptor for egg jelly; TM, transmembrane; TNT, transcription-coupled translation.

10.1021/bi035074c CCC: $25.00
Published on Web 10/14/2003

of their C-terminal sequences to achieve an $N_{cyto}-C_{exo}$ orientation are called type II signal anchors. The simplest, classical model for the topogenesis of a polytopic protein proposes that TM domains are integrated within the ER membrane in a cotranslational and sequential mode and that the initial (or N-terminal-most) hydrophobic segment determines the overall topology of the final protein product (*25*, *26*). Recently, numerous exceptions to this "simple sequential" model of polytopic membrane protein biogenesis have been reported, and the requirements or characteristics involved in these variant methods of membrane insertion are beginning to be elucidated (*27*−*31*).

We set out to determine the number of membrane-spanning segments and the cellular orientation of membrane-flanking regions of polycystin-1. Using a series of N-terminal polycystin TM-glycosylation reporter gene fusions expressed in vivo, N-linked glycosylation of the C-terminal glycosylation reporter was assessed to determine TM domain presence and orientation. The topogenic properties of individual proposed TM domains were also investigated in vitro using a combination of glycosylation, protease protection, and carbonate extraction assays. These studies showed that each of the proposed TM domains, I−XI, from the second polycystin structural model has membrane-spanning capability and thereby provide the first experimental evidence supporting a polycystin-1 11 TM structure.

EXPERIMENTAL PROCEDURES

Construction of Polycystin TM-Glycosylation Reporter Fusion Clones. To generate the series of polycystin TM-glycosylation reporter clones for in vivo transmembrane analysis, a template clone, CD5-12TM-N123S (Figure 1C) was initially created. First, all three potential, native, N-linked glycosylation sites (N3139, N3728, and N3780) within the C-terminal 1284 residues of murine polycystin-1 were removed by mutating asparagine (N) residues conforming to the N-linked consensus sequence, NXS/T, to serine (S) residues. A fourth, atypical site, NPT, at N3348 was also mutated although it was predicted to be nonglycosylated (*32*). This atypical site is not indicated in Figure 1. The sites were mutated by a combination of site-directed mutagenesis (for the N1 site; Gene Editor kit; Promega) and PCR/replacement cloning (for the N2 and N3 sites). All mutations and the integrity of polycystin sequences were confirmed by DNA sequencing. Finally, the C-terminal 1284 residues of polycystin-1 (*Sca*I−*Not*I fragment) were joined in frame with the CD5 protein signal sequence. For the series of clones containing increasing numbers of potential TM domains (Figure 1C), PCR primers complementary to sequences immediately preceding each of the potential TM domains, I−XI and 11 (see Table 1 for TM locations), were designed. Each primer also included an *Eco*RV site and a protection sequence at its 5′ end for use in subsequent cloning (see below for primer sequences). Various portions of the CD5-12TM-N123S template were PCR-amplified using the following primer combinations, confirmed by DNA sequencing, and then joined together using convenient restriction sites. CD5-ΔTM, -I, and -I−II clones used 5′-EcoCD5 and either TMaEcoRV, TMIEcoRV, or TMIIEcoRV primers. CD5-I−III and -I−IV were produced using N1S and either TMIIIEcoRV or TMIVEcoRV primers, followed by *Xma*III/*Eco*RV digestion and ligation into *Xma*III/*Eco*RV-digested CD5-I−II. CD5-I−V and -I−VI were produced using 5′-NPT and either TMVEcoRV or TMVIEcoRV primers, followed by use of the *Xmn*I/*Eco*RV or the *Acc*III/*Eco*RV sites in CD5-I−IV to produce CD5-I−V and CD5-I−VI, respectively. CD5-I−VII, -I−VIII, and -I−IX were produced using fwd381 and either TMVIIEcoRV, TMVIIIEcoRV, or TMIXEcoRV primers followed by subcloning in the 5′ *Eco*RI−*Hin*dIII fragment of CD5-I−VI. CD5-I−X, -I−11, and -I−XI were produced using N3S and either TMXEcoRV, TMXIEcoRV, or TM11EcoRV primers followed by subcloning in the 5′ *Eco*RI−*Xho*I fragment of CD5-I−VI. To join the polycystin TM fragments with the glycosylation reporter, the *Eco*RI−*Eco*RV fragments of CD5-ΔTM through CD5-I−XI clones were ligated into the *Eco*RI and *Bst*EII/end-filled sites of pPS1-HR2 (kindly provided by D. Harris). pPS1-HR2 consists of the first two transmembrane domains of presenilin 1 fused to prolactin (PRL), three N-linked glycosylation consensus sites (N3), and a hemagglutinin (HA) tag in the pcDNA3 vector (Invitrogen) (*33*). *Eco*RI and *Bst*EII digestion removes the presenilin sequences, while end filling of the *Bst*EII site provides a continuous open reading frame between the upstream CD5-polycystin TM fragments and the glycosylation reporter (PRL-N3-HA). The junction between the polycystin and prolactin was confirmed by DNA sequencing with each clone.

To produce the flag- and CD5-single or combined TM-glycosylation reporter constructs for in vitro topogenic studies of TM domains IV, V, X, 11, and XI, the desired N-loop, C-loop, and TM regions were PCR-amplified from appropriate polycystin TM-glycosylation reporter clones using the 5′-loop primers (with incorporated *Eco*RV and *Nru*I sites for subsequent subcloning) and the HAXbaII primer at the 3′ end of the HA epitope within the glycosylation reporter. PCR products were verified by DNA sequencing and then cloned downstream of the CD5 signal sequence or the flag epitope in pBluescript (Stratagene) or pGemT (Promega) vectors.

Primer Synthesis, PCR Reactions, and DNA Sequencing. All primers for mutagenesis, PCR, and DNA sequencing were synthesized at the Kansas Medical Center Biotechnology Support Facility. The primers and their sequences are as follows: N1S, GGAGAGGACAGCCGTAGTG; 5′-NPT, CCTCTTCCGGATGTCTCGGAGTAAGGTGTCTGGAGACCA; N3S, TGGTGCAAAGTGGCTCTGAG; 5′-EcoCD5, TTCTAGAATTCCCTCGACCTCG; fwd381, GCTTCTTGCCATGGTCACGCC; TMaEcoRV, GACTAG**GATATC**GTTGATGCTTGCAGATGGTTC (where the *Eco*RV site is in bold type); TMIEcoRV, GACTAG**GATATC**CCTCTGGACTCTAGTAAAGCG; TMIIEcoRV, GACTAG**GATATC**TGTGTCAACACCAGGAGAGATC; TMIIIEcoRV, GACTAG**GATATC**ATGGGCCAGTGGGGCACACC; TMIVEcoRV, GACTAG**GATATC**AGGGAAGCTGGCACCAATC; TMVEcoRV, GACTAG**GATATC**GTCATGGAGCCTCTTGACCTTTC; TMVIEcoRV, GACTAG**GATATC**AGTGCTGAGTCGCCGTAACG; TMVIIEcoRV, GACTAG**GATATC**GTCAGGCCTTGCTGTGCACG; TMVIIIEcoRV, GACTAG**GATATC**TAGTGAAGCTGCCAGGCCAC; TMIXEcoRV, GACTAG**GATATC**CATGAGCTCGGGCAAGGC; TMXEcoRV, GACTAG**GATATC**GTTGTAGAGAGTGTCAGCACC; TMXIEcoRV, GACTAG**GATATC**GGAAGGCAGTGGATCCATTC; TM11EcoRV, GACTAG**GATATC**GGACAGGTACCAGGACTCAG; HAX-

baII, GACTAG**GTCGAC***TCTAGA*CTATGCGTAATCTGG (with *Sal*I in bold and *Xba*I in italics); loop 3, GACTAG-**GATA*TC***GCGA*GGATGTCTCGGAGTAAGGTGTC (with *Eco*RV in bold and *Nru*I in italics); loop 4, GACTAG-**GATA*TC***GCGA*TCCCTCCCAGCGTGAGTGTC; loop 9, GACTAG**GATA*TC***GCGA*GCAAGACATTGTGTCGGG-CC; loop 10, GACTAG**GATA*TC***GCGA*TTTCCTCTGGT-GCTGACACTC; loop 11, GACTAG**GATA*TC***GCGA*AGTC-CTGGTACCTGTCCCCTC; loop XI, GACTAG**GATA*TC***-GCGA*GTTGGCGGTACCACGCCTTG.

Polymerase chain reactions (PCR) typically included 10 ng of template DNA, 2 mM $MgCl_2$, 250 μM dNTPs, 0.5 μM primers, and 2.5 units of the proofreading Pfu DNA polymerase (Gibco BRL). PCR cycling conditions typically consisted of 2 min initial denaturation at 94 °C, followed by 30 cycles of 1 min at 94 °C, 1 min at appropriate annealing temperature based on primer sequence, and 1−3 min at 72 °C (depending on amplified fragment length), and final extension at 72 °C for 5 min. Big dye DNA sequencing (ABI) was performed by the staff at the Kansas Medical Center Biotechnology Support Facility.

In Vivo Expression and Glycosylation Analyses of Polycystin TM-Glycosylation Reporter Clones. HEK293T cells were maintained in DMEM/4.5 g/L glucose/10% serum with penicillin/streptomycin. For transient transfection of polycystin TM-glycosylation reporter clones, cells were plated at a density of 750000 cells per well in six-well plates ~24 h before incubation with $CaHPO_4$−DNA precipitates. Standard transfection mixtures (for three wells) contained 100 or 250 ng of TM-glycosylation reporter DNA and pBluescript (Stratagene) filler DNA for a total of 8 μg of DNA per reaction. Fresh medium containing 10% serum and no antibiotics was replaced after 3.5 h, and cells were lysed 22−26 h later in 250 μL/well of passive lysis buffer (Promega). For analysis of N-linked glycosylation, membrane sheets in cell lysates were disrupted by addition of detergent to final concentrations of 1% Triton X-100, 0.5% sodium deoxycholate, and 0.1% SDS, and nuclei were pelleted. The supernatant was then mixed with an equal volume of 40 mM phosphate buffer, pH 7.5, 0.1% SDS, and 4 mM EDTA plus protease inhibitors, heated at 65 °C, cooled, and then incubated with, or without, ~0.10 milliunit of *N*-glycosidase F (Glyko)/μg of lysate protein for 16−24 h at 37 °C. Glycosidase reactions or cell lysates were precipitated with methanol, and protein pellets were solubilized in 2× SDS loading buffer by heating at 65 °C (to prevent aggregation of larger fusion proteins) and loaded on either 7.5% or 6% polyacrylamide−SDS minigels with 4% acrylamide stackers. Large format gels (15 cm width × 19 cm length) were used to assay TM I−IX, TM I−X, TM I−11, and TM I−XI fusion proteins. Proteins were electrotransferred to Immobilon-P membrane (Millipore) overnight at 20 V, and blots were blocked in 5% milk−TBSN (10 mM Tris, pH 7.4, 0.9% NaCl, 0.1% NP-40), reacted with a rat anti-HA monoclonal antibody (Roche), followed by an HRP-conjugated anti-rat secondary antibody (Jackson ImmunoResearch), and developed using the chemiluminescence substrate ECL (Amersham). Blots were exposed to film.

In Vitro Expression, Glycosylation, Membrane Integration, and Protease Protection Assays. For in vitro analysis of glycosylation, CD5- or flag-single/combined TM-glycosylation reporter clones (500 ng of DNA/25 μL of reaction) were incubated in coupled transcription/translation (T3-coupled TNT or T7 Quick TNT) extracts (Promega) with 20 μCi of [^{35}S]methionine (Amersham) at 30 °C for 60 min in either the presence or absence of varying amounts of canine pancreatic microsomes (Promega). Addition of microsomal membranes reduced production of fusion protein in a somewhat dose-dependent manner. Therefore, we chose to use an amount of membrane that gave maximal glycosylation with sufficient fusion protein product to enable detection by film within 48 h. For the amount of microsomal membranes used (typically 1−2 μL/25 μL of reaction), it was determined that >60% of the CD5-directed fusion proteins were synthesized on membrane-bound ribosomes. For assessment of membrane association and/or integration, 1 μL of a TNT reaction was equilibrated in 0.5 mL of 100 mM Tris, pH 7.5, and 250 mM sucrose or 100 mM sodium carbonate, pH 11.5 (*34*), respectively, for 30 min, followed by centrifugation for 30 min at 78000 rpm, 4 °C, in a TLA100.2 rotor. Resulting Tris−sucrose supernatants were precipitated in 4 volumes of methanol, and pellets were dissolved in 2× SDS loading buffer and denatured 2 min at 100 °C. Proteins in carbonate buffer supernatants could not be quantitatively precipitated and were therefore not analyzed. Treatment of TNT reactions with *N*-glycosidase F was in glycosylation lysis buffer (150 mM NaCl, 50 mM Tris, pH 7.5, 2 mM EDTA, 0.5% Triton X-100, 0.5% sodium deoxycholate, 0.5% SDS) as described above, typically with 10 μL of reaction. For protease protection analyses, 10 μL of TNT reaction was incubated for 60 min on ice with 50 μg/mL proteinase K in the presence or absence of 1% Triton X-100. Digestion reactions were terminated with 10 mM PMSF and then split and immunoprecipitated with either anti-FLAG affinity beads (Sigma) or anti-prolactin antibody (ICN Biomedical) and protein A beads (Sigma) and then analyzed on either 12% (PRL IP) or 15% (Flag IP) Tris-HCl−polyacrylamide gels. Alternatively, protease digestion samples were split in two and immunoprecipitated with anti-FLAG beads or pelleted in Tris−sucrose buffer with 3 mM PMSF, and the pellets were solubilized and analyzed in 16.5% Tris−Tricine Criterion gels (Bio-Rad). Following electrophoresis, gels were enhanced in 1 M sodium salicylate, dried down, and exposed to film at −70 °C.

RESULTS

Rationale and Construction of Polycystin-TM Glycosylation Reporter Clones. The relative locations of the 11 putative TM domains that were predicted in the first [denoted TM 1−11 (*5*)] and the second [denoted TM I−XI (*7*)] polycystin-1 topology models are illustrated in Figure 1. On the basis of the presence of the REJ domain, the weak hydrophobicity of proposed TM domains 1 and 2 (Figure 1A), and the GPCR proteolytic site (GPS) preceding TM 3/TM I (*18*, *36*), we did not include putative TM domains 1 and 2 in our analysis. Rather, we tested the membrane-spanning ability and the orientation of the proposed TM domains following the GPS domain, specifically, TM I−XI predicted in the second model and TM 11 predicted in the first model. These 12 TM domains are located within the C-terminal 1228 residues of murine polycystin-1. The orthologous amino acid residues comprising these 12 TM domains in human and mouse polycystin-1 are listed in Table 1.

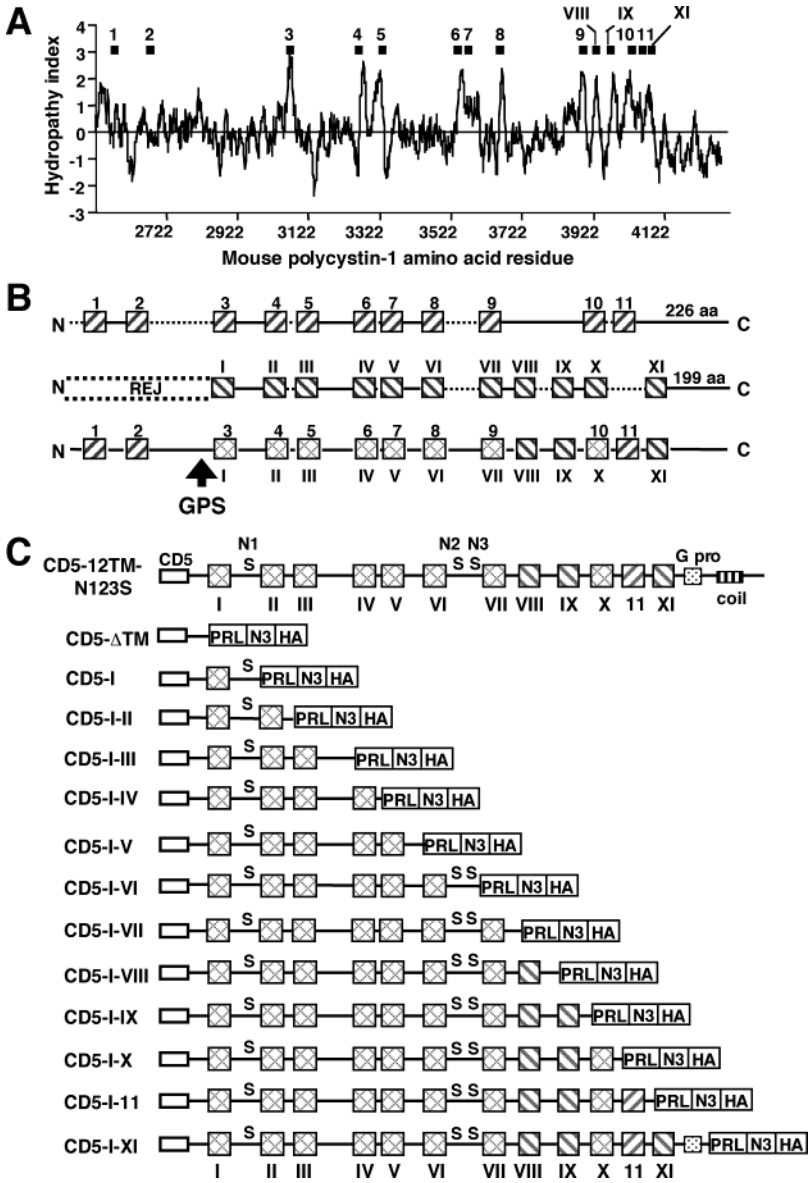

FIGURE 1: Proposed polycystin-1 TM domains and construction of polycystin TM-glycosylation reporter clones. (A) Kyte−Doolittle hydropathy plot (15-residue window) (*35*) of the C-terminal 1772 amino acids of murine polycystin-1 (residues 2522−4293). The locations of putative TM domains proposed in the original (*5*) or the second (*7*) 11 TM structural models are indicated by the bars with Arabic or Roman numerals, respectively. (B) Schematic representation of the relative locations of proposed membrane-spanning domains of polycystin-1. TM domains from the original (top) and the revised (middle) models are indicated by hatched boxes with Arabic or Roman numerals, respectively. The length of the N-terminal extracellular domain increased from 2582 (original model) to 3075 (revised model) residues. The length of the cytosolic C-tail in each model is indicated. Dashed lines indicate proposed extracellular loops. Bottom: composite of the two models. TM domains common to both models are indicated by the crosshatched boxes. Abbreviations: aa, amino acid residues; REJ, receptor for egg jelly domain; GPS, GPCR proteolytic site. (C) Top: polycystin-1 template clone, CD5-12TM-N123S, lacking potential, native N-linked glycosylation sites. The C-terminal 1284 amino acid residues of murine polycystin-1 were cloned in frame following the signal sequence of the CD5 protein. Three consensus N-linked glycosylation sites (N3348, N3728, and N3780), labeled N1, N2, and N3, were removed by mutation of the Asn (N) residue to Ser (S). Bottom: polycystin TM-glycosylation reporter clones used in in vivo glycosylation reporter analyses. Each clone is named for potential TM domain(s) included within its sequences using the Roman numeral nomenclature except for putative TM domain 11. The longest construct, CD5-I−XI, includes the G protein activation domain (G pro) (*17*) and ends after residue 4153/4162 in mouse/human polycystin-1 preceding the coiled-coil domain (coil). Abbreviation: PRL-N3-HA, glycosylation reporter tag.

To test the proposed TM domains of polycystin-1, we employed a glycosylation reporter approach that makes use of classical theories on polytopic membrane protein insertion and the principles of N-linked glycosylation. N-Linked glycosylation occurs within the ER lumen at NXS/T consensus sequences destined to be in extracellular portions of proteins (*37*). N-linked glycosylation increases the molecular mass of the modified protein (~2 kDa for core glycosylation) which can be detected as a shift in electrophoretic mobility of the protein and can be confirmed by *N*-glycosidase F (N-gF) treatment which specifically removes N-linked glycosylation and thereby increases the mobility of the protein. We constructed a series of polycystin-TM clones containing increasing numbers of potential TM domains starting near N-terminal TM domain I.

To produce the polycystin TM-glycosylation reporter constructs, it was necessary to generate an ER-directed, glycosylation-negative polycystin template clone. Therefore,

Table 1: Locations of Putative TM Domains in Human[a] and Mouse[b] Polycystin-1

TM domain	human polycystin-1 (aa)[c]	mouse polycystin-1 (aa)
I	3075−3095	3067−3087
II	3281−3301	3273−3293
III	3323−3343	3315−3335
IV	3559−3579	3550−3570
V	3582−3602	3573−3593
VI	3669−3689	3660−3680
VII	3895−3915	3886−3906
VIII	3934−3953	3925−3944
IX	3994−4014	3985−4005
X	4027−4045	4018−4036
11	4056−4077	4047−4068
XI	4084−4104	4075−4095

[a] GenBank accession number L33243. [b] GenBank accession number NM_013630. [c] Locations as proposed by Sandford et al. (*7*).

the three potential N-linked glycosylation sites within the C-terminal 1284 residues of murine polycystin-1 were mutated (Asn to Ser), and this portion of polycystin was cloned in frame with an N-terminal CD5 signal sequence to generate CD5-12TM-N123S (Figure 1C). This construct served as the template for generating various TM-containing fragments of polycystin by a PCR-based strategy. The first fusion construct, CD5-ΔTM, contained only the proposed extracellular N-terminal region preceding TM I. Each successive polycystin-TM fragment included the next potential TM domain and its associated C-terminal loop region. The longest polycystin-TM construct, CD5-TMI−XI, ended following the G protein activation domain and preceding the coiled-coil domain (Figure 1C). Each polycystin-TM portion was followed by the C-terminal glycosylation reporter cassette. The glycosylation reporter cassette consists of the topologically neutral "spacer segment", the C-terminal 148 residues of prolactin (PRL) (*38*), and is followed by three artificial N-glycosylation consensus sites (N3) and a hemagglutinin (HA) epitope tag.

Glycosylation Analysis of in Vivo Expressed Polycystin-TM Reporter Clones. Transient transfection of 293T cells with CD5-ΔTM through CD5-TMI−XI DNA constructs resulted in production of proteins that were recognized by an anti-HA antibody and were of the expected approximate molecular masses (data not shown). To determine the membrane-spanning potential and orientation of each of the predicted TM domains, we performed glycosylation analyses with the TM-glycosylation reporter fusion proteins (Figure 2A). CD5-ΔTM, which does not encode any of the putative TM domains but includes a portion of the proposed extracellular REJ domain of polycystin preceding TM I, produced several protein species whose electrophoretic mobility increased upon N-gF treatment. The shift in electrophoretic mobility is indicative of N-linked glycosylation of the C-terminal tag and hence of its ER lumenal location. This implies that there were no membrane-spanning or TM domains within this portion of polycystin to prevent translocation of the glycosylation reporter into the ER lumen. CD5-TMI, on the other hand, had the same electrophoretic mobility after treatment with or without N-gF and therefore was not glycosylated. Lack of glycosylation of CD5-TMI implies that this fusion protein contains a functional membrane-spanning domain that prevented translocation of the glycosylation reporter tag into the ER lumen. Furthermore, TM I must have an N-lumenal to C-cytosolic orientation. In contrast, the slower migrating TM I−II protein species observed in the absence of N-gF was eliminated by treatment with glycosidase, demonstrating that the multiple banding pattern was due to N-linked glycosylation of the reporter tag. Therefore, the TM I−II fusion protein must contain an additional TM domain with an N-cytosolic/C-lumenal orientation that results in translocation of the reporter tag into the ER lumen for a portion of the fusion protein synthesized. Presumably, the multiple glycosylated species observed for TM I−II were due to modification of one, two, or all three N-linked glycosylation sites in the reporter.

N-gF treatment of the lysates from the TM I−III, TM I−V, TM I−VII, TM I−IX, and TM I−XI transfected cells had no effect on the mobility of these fusion proteins (Figure 2A). As with TM I−II, multiple protein bands were observed for TM I−IV and TM I−VIII fusion proteins in the absence of N-gF. Glycosidase treatment eliminated the most slowly migrating bands and increased the intensity of the band with the greatest mobility for both TM I−IV and TM I−VIII. In contrast, TM I−VI fusion protein consisted of a single protein species whose mobility was increased by N-gF treatment. As for TM I−X and TM I−11 fusion proteins, only very faint bands migrating slower than the major protein band were visible and were eliminated by glycosidase treatment. These results indicate that fusion proteins terminating in the loop regions following transmembrane domains II, IV, VI, VIII, X, and 11 are capable of being glycosylated (to different extents), while those following TM domains I, III, V, VII, IX, and XI were not glycosylated. Since the pattern of absence or presence of N-linked glycosylation alternated with the addition of each putative TM domain with the exception of TM 11, this analysis suggests that each of the TM domains proposed in the second topology model (i.e., TM I−XI) is a functional membrane-spanning domain.

Reduced Expression Levels Affect Glycosylation Status of Some Glycosylation Reporter Proteins. Polycystin TM-glycosylation reporter fusion proteins terminating in the loop regions following TM II, IV, VIII, X, and 11 consisted of both glycosylated and nonglycosylated species when expressed in vivo. Such results are indicative of multiple topogenic forms that could be due to misfolding or misintegration of the fusion protein, to alternative conformations, or to disruption of a topogenic signal. We could rule out steric hindrance of glycosylation since each fusion protein had the same C-terminal N-linked glycosylation consensus sites following the topologically neutral prolactin spacer segment. It was also possible that overexpression of these fusion proteins overwhelmed the glycosylation machinery of the 293T cells and thus prevented modification of all polypeptides. To address the latter possibility, we reduced the expression level of the TM I−II fusion protein by transfecting lower amounts of DNA, or by cycloheximide or actinomycin D treatment, and assayed the effect on glycosylation status (Figure 2B). Actinomycin D treatment resulted in decreased amounts of both glycosylated and nonglycosylated TM I−II fusion protein species, while cycloheximide treatment resulted in an enrichment of the glycosylated forms relative to the nonglycosylated species. Importantly, transfection with 1 ng of CD5-TMI−II DNA/reaction mix resulted in fusion protein that consisted entirely of glycosylated species. Thus, transfection with low DNA

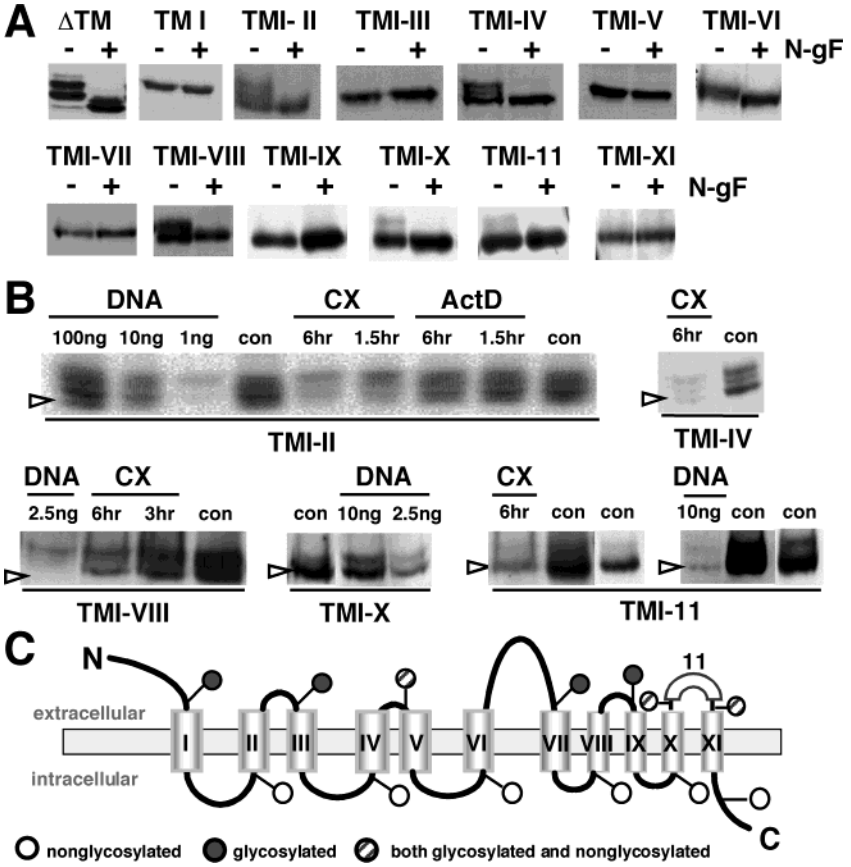

FIGURE 2: In vivo expression and glycosylation reporter analyses. (A) Anti-HA Western blots of lysates from cells transiently transfected with the various polycystin TM-glycosylation reporter clones and incubated either with (+) or without (−) *N*-glycosidase F (N-gF). Lysates from mock-transfected cells did not react with the HA antibody (data not shown). TM I−IX, TM I−X, TM I−11, and TM I−XI fusion proteins were analyzed on large format gels. Fusion proteins ΔTM, TM I−II, TM I−IV, TM I−VI, TM I−VIII, TM I−X, and TM I−11 were glycosylated to different extents. Multiple bands for ΔTM, TM I−II, TM I−IV, and TM I−VIII fusion proteins in the absence of N-gF are presumed to be due to N-glycosylation at one, two, and or all three sites within the glycosylation reporter. (B) Anti-HA Western blot analyses of lysates from cells transfected with varying amounts of fusion protein DNA or with 250 ng of fusion protein DNA (con) and treated with cycloheximide (CX) or actinomycin D (ActD) for 1.5, 3, or 6 h prior to harvest. The open arrowhead in each blot indicates the nonglycosylated form of the fusion protein. Both long and short (rightmost lane) exposures are shown for the CX and DNA controls for TM I−11. The CX and DNA results for TM I−11 are from different gels. Reduced expression conditions completely converted TM I−II and TM I−VIII to glycosylated species and slightly improved the relative amount of glycosylated to nonglycosylated forms for TM I−IV, TM I−X, and TM I−11. (C) Summary of glycosylation reporter analyses and supported model of membrane-associated structure of polycystin-1. Predicted TM domains are represented by numbered cylinders. Ball and stick represent locations and glycosylation status of the C-terminal glycosylation reporter in the various polycystin TM-glycosylation reporter fusion proteins. Key: open ball, nonglycosylated reporter; filled ball, glycosylated reporter; hatched ball, both glycosylated and nonglycosylated reporter.

amounts and/or cycloheximide treatment was performed with all polycystin-TM glycosylation reporter constructs. Transfection of lower DNA amounts resulted in complete conversion of TM I−VIII fusion protein to glycosylated forms (Figure 2B). Neither cycloheximide treatment nor lower DNA amounts completely converted TM I− IV, TM I−X, or TM I−11 fusion proteins to glycosylated forms but did appear to increase the relative amounts of the glycosylated species. Similar treatments were performed with the remainder of the fusion protein constructs, and their glycosylation status did not change with reduced expression levels (data not shown). The results of these glycosylation reporter analyses are superimposed on a topologic model of polycystin-1 based on interpreting any level of glycosylation as a lumenal location of the glycosylation reporter (Figure 2C). Since lower expression levels of most of the glycosylation reporter constructs resulted in either nonglycosylated or glycosylated species, it appears that the production of both species with reporter constructs TM I−IV, TM I−X, and TM I−11 was due to something other than overexpression, perhaps disruption of the structure of polycystin by the location of the C-terminal truncation, or weak or incomplete topogenic information within these TM domains and their associated loop regions. The latter alternative implies that these TM domains require the presence of additional, C-terminal domains in order to efficiently integrate into the ER membrane. These possibilities were addressed in the following experiments that assayed the topogenic properties of TM domains IV, V, X, 11, and XI in isolation and in series.

Topogenic Properties of TM Segments IV and V. To determine if proposed TM domains IV and V contained inherent stop transfer activity that was capable of preventing translocation of C-terminal sequences and directing membrane integration, TM IV or TM V and their respective N- and C-loop regions were fused to the C-terminal glycosylation reporter tag (PRL-N3-HA) and the N-terminal CD5 signal sequence (Figure 3A). A signal sequence was added in order to direct the synthesis of these fusion proteins on microsome-bound ribosomes. The constructs were expressed

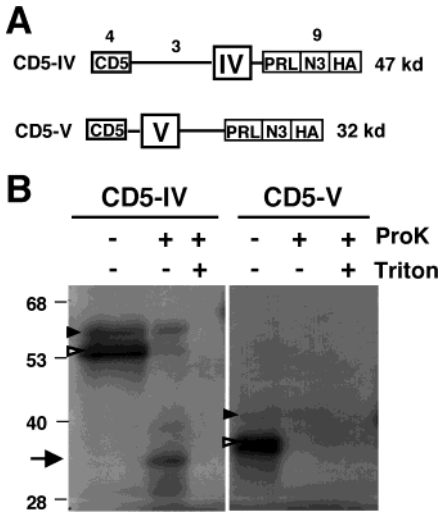

FIGURE 3: Stop transfer capability of individual TM IV and TM V domains. (A) Illustration of CD5-IV and CD5-V single TM-glycosylation reporter constructs. TM IV or TM V and their associated N- and C-loop regions were cloned in frame with an N-terminal signal sequence (CD5) and a C-terminal glycosylation reporter tag (PRL-N3-HA). Predicted molecular masses of the nonglycosylated product are indicated to the right of each construct. The number of methionine residues is shown above the corresponding segment in the CD5-IV construct. (B) Proteinase K sensitivity analysis of CD5-IV and CD5-V. Fusion proteins produced in TNT extracts supplemented with canine pancreatic microsomes were treated with proteinase K (ProK) in the absence (−) or presence (+) of Triton to assay for protection of full-length fusion protein. Glycosylated species were determined by N-gF assays (data not shown): open arrowhead, nonglycosylated full-length fusion protein; filled arrowhead, glycosylated full-length fusion protein; arrow, protected fragment of CD5-IV. Full-length CD5-IV always migrated with a larger apparent molecular weight than predicted. Both fusion proteins appear as doublets in the presence of microsomal membranes. The bottom band may represent signal sequence cleavage of the fusion protein. Greater than 60% of the fusion proteins were determined to be synthesized on microsome-bound membranes (data not shown). Only minor amounts of CD5-IV and CD5-V were glycosylated and protease-protected, while the majority of both fusion proteins were digested by protease in intact microsomes.

in in vitro coupled transcription/translation (TNT) extracts in the presence or absence of rough microsomal membranes and assayed for glycosylation status and protease sensitivity in order to distinguish between translocation and membrane integration (Figure 3B). The functionality of the CD5 signal sequence was demonstrated by pelleting of the TNT plus microsome reactions through neutral Tris−sucrose cushions which resulted in the majority of each fusion protein being present in the membrane pellet (data not shown). N-gF treatment showed that a significant amount of CD5-IV was glycosylated, while only a very minor portion of CD5-V was glycosylated (data not shown). Proteinase K digestion of CD5-IV in the presence of intact microsomal membranes (i.e., without Triton) resulted in the protection of the full-length, glycosylated fusion protein and a shorter protein species, while neither form was protected from protease in the presence of Triton X-100. The shorter product was approximately the size expected for an N-terminal fragment consisting of the preceding loop and TM IV. Taking into account the number of labeled methionines (Met) within a protease-protected N-terminal fragment (7 Met) versus the full-length fusion protein (16 Met total), it was determined that the predominant form of CD5-IV was a membrane-integrated form. For CD5-V, the vast majority of the fusion protein was digested, and only a minor amount of the full-length, glycosylated protein was protected from protease digestion in intact microsomes. These results demonstrate that both TM IV and TM V have stop translocation activity.

To determine if TM domains IV or V contain inherent signal sequence or signal anchor determinants capable of directing synthesis on microsomal membrane-bound ribosomes and/or directing integration and orientation within membranes, fusion constructs lacking the N-terminal CD5 signal sequence were made. TM IV or TM V and their respective associated loop regions were fused to the C-terminal glycosylation reporter tag (PRL-N3-HA) and an N-terminal flag epitope tag (Figure 4A) and were expressed in TNT extracts with or without microsomal membranes. Association with microsomal membranes was assayed by centrifuging translation products in a neutral Tris−sucrose buffer. Alkaline carbonate extraction followed by centrifugation was used to distinguish between lumenal/peripheral versus integral membrane fusion proteins (Figure 4B). And finally, glycosylation status (data not shown) and protease protection assays were used to assign orientation of membrane-integrated fusion proteins (Figure 4C). The Tris centrifugation assays demonstrated that approximately half of the flag-IV and flag-V fusion protein products were associated with the microsomal membranes (compare the amount of fusion protein in the pellet versus the supernatant). The carbonate centrifugation assays showed that all of the fusion protein that was associated with the microsomal membrane pellet was also integrated. Notably, the membrane-associated flag-IV was enriched in the glycosylated form of the fusion protein, as determined by glycosidase treatment (data not shown), suggesting that TM IV was not only able to direct its synthesis on membrane-bound ribosomes but was also able to direct translocation of its C-terminus. In contrast, flag-V, which was predominantly nonglycosylated (data not shown), was also able to direct its synthesis on membrane-bound ribosomes but prevented translocation of the C-terminal glycosylation reporter tag.

To confirm the preceding membrane integration and orientation interpretations, protease digestion of flag-IV and flag-V fusion proteins followed by immunoprecipitation with antibody against either the N-terminal flag or the C-terminal PRL epitope was performed (Figure 4C). These experiments resulted in protection of a C-terminal, anti-PRL-precipitable fragment for flag-IV but lack of protection of an N-terminal, anti-flag precipitable fragment. The protected C-terminal fragment for flag-IV was larger than predicted for the unmodified TM IV-reporter tag portion and was most likely due to glycosylation of the reporter tag. For flag-V, protease digestion did not yield a protected C-terminal PRL fragment, as was anticipated on the basis of the lack of glycosylation and the centrifugation results above. An expected protease-protected N-terminal fragment consisting of the flag epitope and TM V together was not detectable, most likely due to lack of resolution of such a small peptide (~4 kDa) in the Tris-HCl gel system. To address this issue, protease digestion reactions of flag-V were split in two, and each half-reaction was either anti-flag immunoprecipitated or pelleted in Tris−sucrose buffer and then electrophoresed on Tris−Tricine gels.

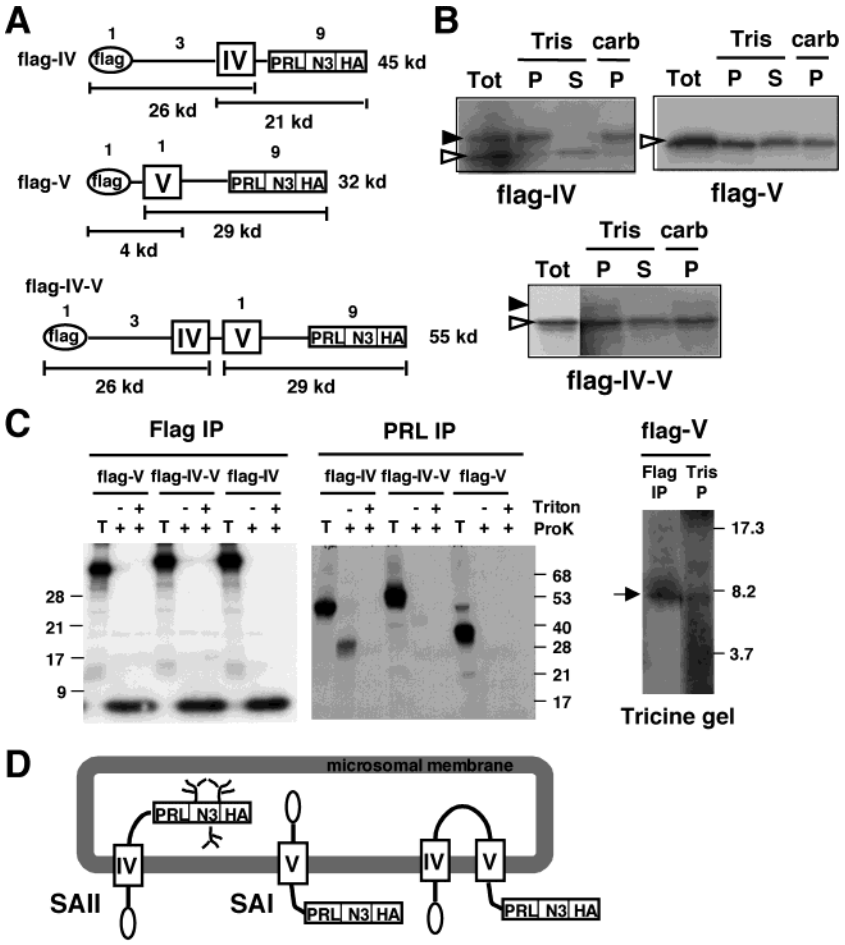

FIGURE 4: Signal anchor analysis of TM IV and TM V. (A) Illustration of flag-IV, -V, and -IV−V glycosylation reporter constructs. Each construct consists of an N-terminal flag epitope followed by TM domains IV, V, or IV and V with their associated N- and C-loop regions and a C-terminal glycosylation reporter tag (PRL-N3-HA). Predicted molecular masses of the unmodified full-length fusion protein and N- and C-terminal fragments are indicated. The number of methionine residues are shown above the corresponding segment in each construct. (B) Membrane association/integration of the flag-IV, -V, and -IV−V proteins. Fusion proteins were produced in TNT extracts supplemented with canine pancreatic microsomes (Tot), and equal aliquots were subjected to centrifugation through a Tris−sucrose (Tris) or an alkaline carbonate (carb) buffer. Glycosylated species were determined by N-gF assays (data not shown). Abbreviations: P, pellet fraction; S, supernatant fraction. Key: open arrowhead, nonglycosylated fusion protein; filled arrowhead, glycosylated fusion protein. Approximately half of each of the fusion proteins was present in the Tris−sucrose and carbonate pellets. Pellet-associated flag-IV was mostly glycosylated, while pellet-associated flag-V and flag-IV−V were largely nonglycosylated. (C) Proteinase K protection analysis of flag-IV, flag-V, and flag-IV−V. Fusion proteins were produced in TNT extracts supplemented with canine pancreatic microsomes and were treated with ProK in the absence (−) or presence (+) of Triton. Equal aliquots of the ProK reactions were immunoprecipitated with anti-flag (Flag IP) or anti-prolactin (PRL IP) antibodies and analyzed on Tris-HCl gels (left two panels) along with untreated, immunoprecipitated fusion protein (T). Bands at the bottom of the Flag IP gel represent protease-resistant peptide fragments that migrated just above the dye front in all samples. C-terminal, PRL-containing and N-terminal, flag-containing fragments were protease-protected for flag-IV and flag-V, respectively. Neither epitope was protected for flag-IV−V. In a separate experiment, ProK-digested flag-V fusion protein was either flag-immunoprecipitated (Flag IP) or centrifuged through Tris−sucrose (Tris P), and the resulting pellets were analyzed on a Tris−Tricine gel (right panel). An ~8 kDa protease-protected flag-containing fragment (arrow) was also present in the Tris−sucrose pellet, indicating lumenal location. This fragment migrated at roughly twice its expected molecular mass, as was observed for other small flag-containing marker proteins (data not shown), which was presumably due to the highly charged flag epitope. (D) Interpretation of the membrane association and protease protection assays. The membrane topology of the flag-TM-glycosylation reporter fusion proteins are illustrated with respect to the microsomal membrane. N3 is shown as glycosylated for flag-IV. Abbreviations: SAI, signal anchor type I; SAII, signal anchor type II.

In these experiments, we detected a flag-precipitable protease-resistant fragment that was also present in the membrane pellet (Figure 4C). The flag-containing fragment was larger than predicted, which was most likely due to the highly charged nature of the flag epitope. Tricine gel electrophoresis of various flag-containing marker proteins also showed aberrant mobilities and increased apparent molecular masses (data not shown). Together, these experiments demonstrate that TM IV has signal anchor type II activity (C-terminus translocation) while TM V has signal anchor type I activity (N-terminus translocation), as illustrated in Figure 4D. These results are consistent with TM IV and TM V functioning as a pair of membrane-spanning domains.

To confirm our assignment of TM IV and TM V as a TM domain pair, we assessed the membrane association and the topology of a flag-TM-glycosylation reporter fusion construct containing both TM IV and V domains (flag-IV−V; Figure 4A). Centrifugation analyses of flag-IV−V in Tris−sucrose or carbonate buffer demonstrated that most of the fusion protein was integrated within microsomal membranes (Figure 4B) and only a minor amount of the membrane-associated protein was glycosylated (data not shown). Proteinase K

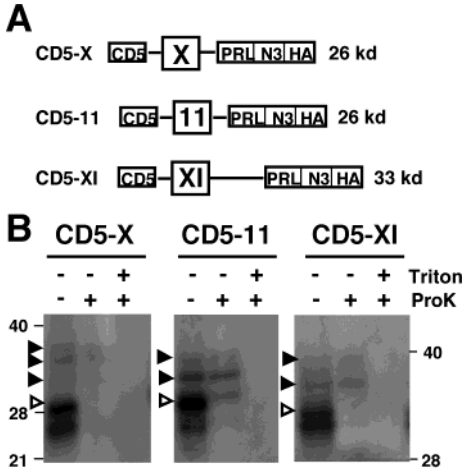

FIGURE 5: Stop transfer capability of individual TM X, TM 11, and TM XI domains. (A) Illustration of CD5-X, -11, and -XI single TM-glycosylation reporter constructs. TM X, TM 11, or TM XI and their associated N- and C-loop regions were cloned in frame with an N-terminal signal sequence (CD5) and a C-terminal glycosylation reporter tag (PRL-N3-HA). Predicted molecular masses of nonglycosylated products are indicated to the right of each construct. (B) Proteinase K sensitivity analysis of CD5-X, -11, and -XI. Fusion proteins were produced in TNT extracts supplemented with canine pancreatic microsomes and were treated with ProK in the absence (−) or presence (+) of Triton to assay for protection of the full-length fusion protein. Glycosylated species were determined by N-gF assays (data not shown). Key: open arrowhead, nonglycosylated full-length fusion protein; filled arrowhead, glycosylated full-length fusion protein. The majority of the fusion proteins were determined to be synthesized on microsome-bound ribosomes as detailed in Experimental Procedures (data not shown). The band below each of the nonglycosylated full-length fusion proteins was observed in TNT reactions with microsomes and may represent the signal peptide-cleaved form of the fusion protein. Only minor amounts of CD5-X and CD5-XI were glycosylated and protease-protected, while the majority of these fusion proteins were protease-sensitive. Relatively more CD5−11 was glycosylated and protease-protected.

digestion followed by anti-flag or anti-PRL immunoprecipitation resulted in complete lack of protected fragments (Figure 4C), suggesting that both the N- and C-termini were cytosolic as illustrated in Figure 4D.

Topogenic Properties of TM Segments X, 11, and XI. To determine if proposed TM domains X, 11, or XI possessed inherent stop translocation and membrane integration properties, TM X, TM 11, or TM XI and their associated N- and C-loop regions were fused with the N-terminal signal sequence (CD5) and the C-terminal glycosylation reporter tag (PRL-N3-HA) (Figure 5A). The constructs were expressed in TNT extracts in the presence or absence of microsomal membranes and assayed for glycosylation status (data not shown) and for protease sensitivity (Figure 5B). Both CD5-X and CD5-XI produced only minor amounts of glycosylated full-length fusion protein that was protease-protected in intact microsomes while the majority of fusion protein was digested, suggesting that both TM X and XI have stop transfer activity and spanned the microsomal membrane. CD5-11, on the other hand, produced relatively more glycosylated, protease-protected full-length product, suggesting that TM11 lacks, or has very weak, stop transfer determinants.

To determine if TM segments X, 11, and XI contain inherent signal sequence or signal anchor activity, they were subcloned as flag-TM-glycosylation reporter fusion constructs (Figure 6A), were produced in TNT extracts in the presence of microsomal membranes, and were subjected to centrifugation through Tris−sucrose or carbonate buffer (Figure 6B). For both TM X and TM 11 flag fusions, at least half of the fusion protein product was found in the Tris−sucrose supernatant, suggesting that these segments have weak signal sequence activity. Notably, none of the flag-11 fusion protein present in the Tris pellet was glycosylated and only a trace amount was detected in the carbonate pellet, thus indicating that flag-11 was peripherally associated with the cytosolic side of the microsomal membrane. Carbonate extraction demonstrated that the fraction of flag-X that was associated with the microsomes (Tris pellet) was also integrated within the membrane. Approximately half of the integrated flag-X was glycosylated, indicating that TM X was able to translocate its C-terminus and thus has inherent signal anchor type II activity. In contrast, the majority of flag-XI fusion protein pelleted in both the Tris−sucrose and carbonate buffers, indicating both microsomal synthesis and integration within the membrane. The majority of membrane-integrated flag-XI was nonglycosylated, suggesting that TM XI largely prevented translocation of the C-terminal glycosylation reporter and thus has predominant signal anchor type I activity.

To confirm membrane integration and orientation, flag-X, flag-11, and flag-XI fusion proteins were assayed for protease-protected fragments. Protease digestion of the flag-X fusion protein followed by anti-flag immunoprecipitation (Figure 6C) resulted in protection of a minor amount of full-length, glycosylated flag-X, while anti-PRL precipitation yielded a fragment consistent in size with a glycosylated form of a C-terminal fragment. Protease digestion of flag-11 (Figure 6C) did not yield any protected flag- or PRL-precipitable fragments. Protease digestion and anti-flag precipitation of flag-XI fusion protein yielded some full-length glycosylated fusion protein and a fragment of unexpected size (for a flag-loop-TM XI containing fragment) that was also present in the Triton-treated sample (Figure 6C). The latter species may represent a protease-resistant flag-containing fragment with unusual electrophoretic mobility. Anti-PRL immunoprecipitation of protease-digested flag-XI resulted in protection of only a minor amount of full-length, glycosylated flag-XI.

To determine if any of the protease-resistant flag-containing fragments represented intraluminal protease-protected N-terminal fragments, protease digestion reactions for flag-X, flag-11, and flag-XI were split, and each half-reaction was either immunoprecipitated with anti-flag or pelleted in Tris−sucrose buffer and analyzed on Tris−Tricine gels. For all three fusion proteins, protease-resistant, anti-flag-precipitable fragments of various sizes were detected (Figure 6D); however, the protease-resistant flag fragment from flag-XI was the only one that was also present (and enriched) in the Tris−sucrose pellet from intact microsomes (−Triton). Altogether, these results demonstrate that TM X has signal anchor type II determinants and TM XI has inherent signal anchor type I activity, while TM 11 (or loop 11) is not integrated within but may be peripherally associated with the membrane (Figure 6E).

Membrane Topogenesis of TM X−XI. Since the preceding topogenic assays suggested that predicted TM 11 may be

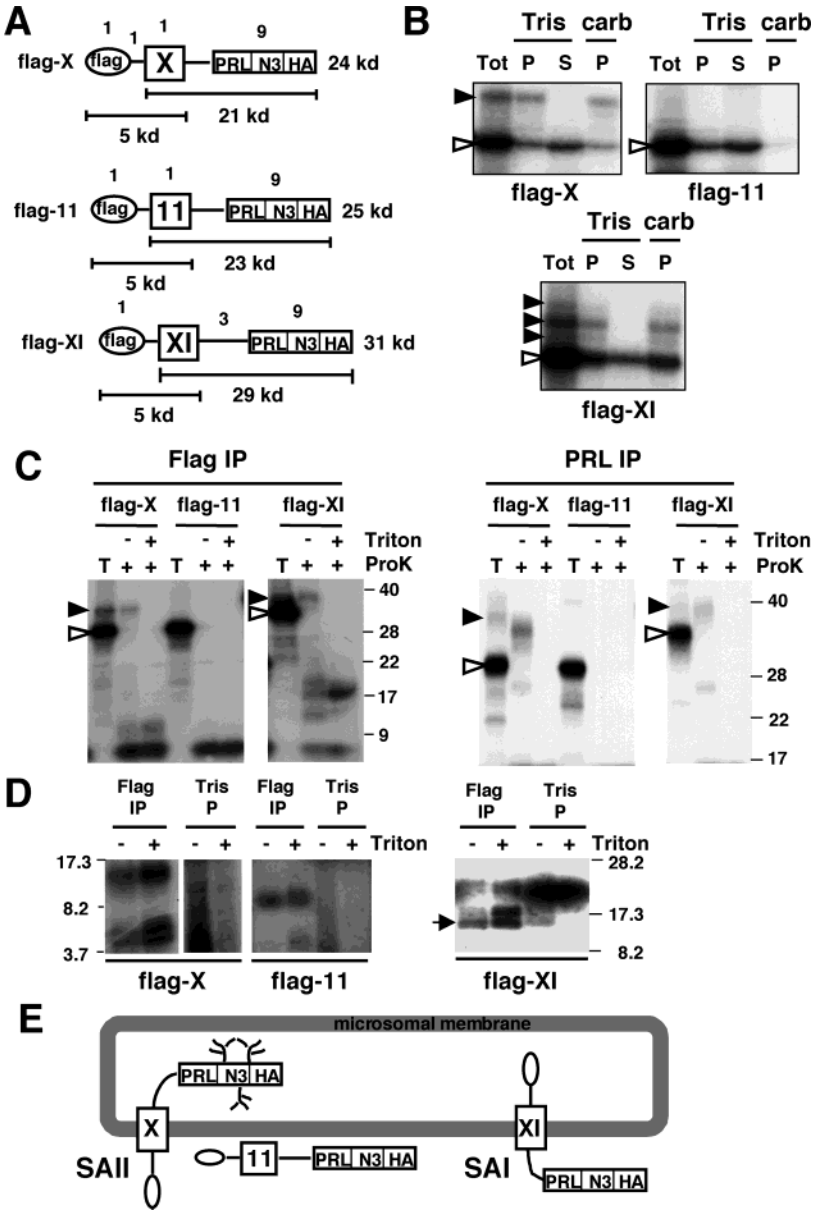

FIGURE 6: Signal anchor analysis of individual TM domains X, 11, and XI. (A) Illustration of flag-X, -11, and -XI glycosylation reporter fusion proteins. Each construct consists of an N-terminal flag epitope followed by TM domains X, 11, or XI with their associated N- and C-loop regions and a C-terminal glycosylation reporter tag (PRL-N3-HA). Predicted molecular masses of the unmodified full-length protein and N- and C-terminal fragments are indicated. The number of methionine residues is shown above the corresponding segment in each construct. (B) Membrane association/integration of the flag-X, -11, and -XI proteins. Fusion proteins were produced in TNT extracts supplemented with canine pancreatic microsome (Tot), and equal aliquots were subjected to centrifugation through a Tris−sucrose (Tris) or an alkaline carbonate (carb) buffer. Glycosylated species were determined by N-gF assays (data not shown). Abbreviations: P, pellet fraction; S, supernatant fraction. Key: open arrowhead, nonglycosylated fusion protein; filled arrowhead, glycosylated fusion protein. Flag-11 was not glycosylated and did not pellet in carbonate buffer, while only a minor amount was detected in the Tris−sucrose pellet. The portion of flag-X present in the Tris and carbonate pellets was enriched in glycosylated forms. The majority of flag-XI was present in both Tris and carbonate pellets and was mostly nonglycosylated. (C) Proteinase K protection analysis of flag-X, flag-11, and flag-XI. Fusion proteins were produced in TNT extracts supplemented with canine pancreatic microsomes and were treated with ProK in the absence (−) or presence (+) of Triton. Equal aliquots of the ProK reactions were immunoprecipitated with anti-flag (Flag IP) or anti-prolactin (PRL IP) antibodies and analyzed on Tris-HCl gels along with untreated, immunoprecipitated fusion protein (T). Bands at the bottom of the Flag IP gel represent protease-resistant peptide fragments that migrated just above the dye front. Key: open arrowhead, nonglycosylated fusion protein; filled arrowhead, glycosylated fusion protein. C-terminal, PRL-containing and N-terminal, flag-containing fragments were protease-protected for flag-X and flag-XI proteins, respectively. No epitope-containing fragments were protease-protected for flag-11. (D) Assessment of lumenal location of protease-resistant flag fragments. Fusion proteins produced in TNT extracts with microsomes were treated with ProK in the absence (−) or presence (+) of Triton. Equal aliquots of the ProK reactions were anti-flag-immunoprecipitated (Flag IP) or centrifuged through Tris−sucrose (Tris P), and the resulting pellets were analyzed on Tris−Tricine gels. Only flag-XI yielded a protease-resistant flag fragment that was also present in the Tris pellet (arrow). This fragment migrated at a larger than expected molecular mass, as did other small flag-containing marker proteins (data not shown), presumably due to the highly charged flag epitope. (E) Interpretation of membrane association and protease protection assays. The membrane topology of the flag-TM-glycosylation reporter fusion proteins is illustrated with respect to the microsomal membrane. N3 is shown as glycosylated for flag-X. Abbreviations: SAI, signal anchor type I; SAII, signal anchor type II.

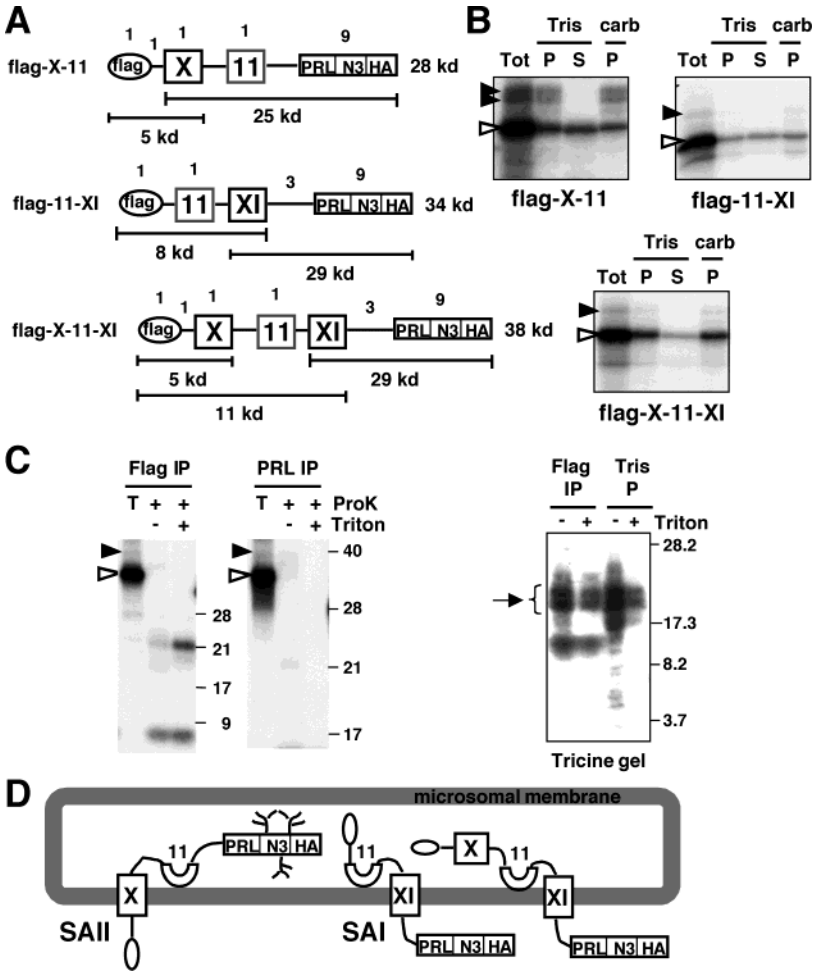

FIGURE 7: Membrane topology and biogenesis of C-terminal TM domains. (A) Illustration of flag-X−11, -11−XI, and -X−11−XI glycosylation reporter fusion proteins. Each construct consists of an N-terminal flag epitope followed by combinations of TM domains X and XI and loop 11 along with their associated N- and C-loop regions and a C-terminal glycosylation reporter tag (PRL-N3-HA). Predicted molecular masses of the unmodified full-length protein and N- and C-terminal fragments are indicated. The number of methionine residues is shown above the corresponding segment in each construct. (B) Membrane association/integration of the flag-X−11, -11−XI, and -X−11−XI fusion proteins. Fusion proteins were produced in TNT extracts supplemented with canine pancreatic microsomes (Tot), and equal aliquots were subjected to centrifugation through a Tris−sucrose (Tris) or an alkaline carbonate (carb) buffer. Glycosylated species were determined by N-gF assays (data not shown). Abbreviations: P, pellet fraction; S, supernatant fraction. Key: open arrowhead, nonglycosylated fusion protein; filled arrowhead, glycosylated fusion protein. Addition of loop 11 sequences increased the amount of flag-X−11 and flag-X−11−XI in the Tris and carbonate pellets and appeared to decrease the relative amount of flag-11−XI in the pellets. Pellet fractions of flag-X−11 were enriched in glycosylated forms, while pelleted flag-11−XI and flag-X−11−XI were primarily nonglycosylated. (C) Proteinase K protection analysis of flag-X−11−XI. Left two panels: Fusion protein was produced in TNT extracts with microsomes and was treated with ProK in the absence (−) or presence (+) of Triton. Equal aliquots of the ProK reactions were immunoprecipitated with anti-flag (Flag IP) or anti-prolactin (PRL IP) antibodies and analyzed on Tris-HCl gels along with untreated, immunoprecipitated fusion protein (T). Only N-terminal, flag-containing fragments were resistant to protease digestion. Right panel: To assess the location of protease-resistant flag fragments, flag-X−1−XI fusion protein produced in TNT extracts with microsomes was treated with ProK in the absence (−) or presence (+) of Triton. ProK reactions were either anti-flag-immunoprecipitated (Flag IP) or centrifuged through Tris−sucrose (Tris P), and the resulting pellets were analyzed on Tris−Tricine gels. Two protease-resistant N-terminal flag-containing fragments (bracket and arrow) were enriched in the Tris pellet in the absence of Triton. The flag-containing fragments migrated at a larger than expected molecular mass, as did other small flag-containing marker proteins (data not shown), presumably due to the highly charged flag epitope. (D) Interpretation of membrane association and protease protection assays. The membrane topology of flag-TM-glycosylation reporter fusion proteins are illustrated with respect to the microsomal membrane. N3 is shown as glycosylated in flag-X−11. Abbreviations: SAI, signal anchor type I; SAII, signal anchor type II.

part of an extracellular loop (loop 11) between TM domains X and XI, we investigated whether the addition of "loop 11" influenced the topogenic properties of either TM X or TM XI alone, or together. Flag-TM-glycosylation reporter fusion constructs consisting of TM X-loop 11, loop 11-TM XI, or TM X-loop 11-TM XI were made (Figure 7A) and tested for their membrane association/integration and orientation as above. Tris−sucrose and carbonate extraction assays showed that flag-X-11 was associated with, and integrated within, the microsomal membranes (Figure 7B). Addition of loop 11 sequences appeared to increase the membrane association of TM X as shown by the approximately equal distribution of flag-X−11 in the Tris−sucrose pellet and supernatant fractions (compare to Figure 6B). As observed for flag-X alone, both the Tris and carbonate pellets were enriched in the glycosylated form of flag-X−11, consistent with a C-lumenal integrated orientation and therefore signal anchor type II activity for TM X-loop 11 (as illustrated in Figure 7D). The assignment of a signal anchor type II activity for flag-X−11 was confirmed by protease digestion experi-

ments which showed protection of a PRL-containing fragment consistent with the glycosylated form of the C-terminal portion of flag-X−11 (data not shown). Addition of loop 11 sequences to TM XI appeared to decrease slightly the membrane association and integration of flag-11−XI (Figure 7B) but did not change its membrane topology. As was seen for flag-XI alone, the vast majority of membrane-integrated flag-11−XI fusion protein was nonglycosylated, consistent with a predominant signal anchor type I orientation (Figure 7D).

Most interestingly, the presence of both TM X and XI along with loop 11 in the flag-X−11−XI fusion construct dramatically increased the membrane association and integration of this fusion protein as shown by the vast majority of fusion protein present in the pellet fractions from the Tris−sucrose and carbonate centrifugation assays (Figure 7B). Very little of the membrane-integrated flag-X−11−XI fusion protein was glycosylated, consistent with a predominantly cytoplasmic location of the C-terminal glycosylation reporter. To determine the topology of flag-X−11−XI within the microsomal membranes, protease digestion followed by anti-flag and anti-PRL immunoprecipitation was performed. In the presence of intact microsomal membranes, both the anti-flag and anti-PRL immunoprecipitates contained a minor amount of full-length, glycosylated fusion protein (Figure 7C). No PRL-containing fragments were protected, confirming that the majority of the C-terminus is cytosolic. However, a series of anti-flag immunoprecipitable fragments were produced in both the absence and presence of Triton, suggesting that the N-terminus of flag-X−11−XI has an unusual conformation or sequence content that is protease-resistant. Similar protease-resistant, anti-flag precipitable fragments of smaller size were also observed for flag-XI (Figure 6C) and flag-11−XI (data not shown). To determine if the N-terminus of flag-X−11−XI was lumenal, protease digestion reactions were either immunoprecipitated with anti-flag or pelleted in Tris−sucrose buffer and separated on Tris−Tricine gels (Figure 7C). Protected fragments with a similar pattern and mobility as those immunoprecipitated with the flag antibody were enriched in the Tris−sucrose pellet in the absence of Triton. Together, these results demonstrate that flag-X−11−XI has an N-lumenal and C-cytosolic orientation (Figure 7D). Surprisingly, although TM X had signal anchor type II activity (albeit weak) in both flag-X and flag-X-11 fusion proteins, TM X did not appear to integrate within the membrane in the flag-X−11−XI fusion protein. This latter observation together with the increased efficiency of membrane association and integration of TM X-loop 11-TM XI suggests that multiple topogenic determinants may be required to achieve the correct membrane topology of these C-terminal TM domains of polycystin-1.

DISCUSSION

We have obtained data supporting the 11 TM domain model proposed by Sandford et al. (*7*) for polycystin-1. The membrane-spanning ability and the orientation of proposed TM domains following the REJ and GPS domains were tested using a series of polycystin TM-glycosylation reporter fusion proteins. The fusion proteins started with the loop region before TM I and added subsequent C-terminal TM domains (Figure 1C). Since associated loop regions have been shown in some cases to influence the membrane orientation of TM domains (*39*; i.e., the charge difference rule), both N- and C-terminal loop regions with their associated TM domains were included in order to have complete topogenic information present. Each construct ended in a C-terminal glycosylation reporter tag, PRL-N3-HA. This type of strategy has been successfully used to analyze topology in other proteins (*27*, *29*, *31*, *40*). The results of glycosylation reporter analyses were unambiguous for the majority of the TM domains tested (Figure 2A). The level of overexpression of the fusion proteins affected the efficiency of N-linked glycosylation within the 293T cells (Figure 2B). Attempts to use cell lines with more prominent modification systems (i.e., pancreatic cell lines) were thwarted by their very low level of transfection efficiency (data not shown). The first glycosylation reporter fusion protein which contained the GPS domain and a portion of the REJ domain preceding TM I was glycosylated, while the addition of TM I prevented translocation of the reporter sequence. Assignment of TM I as the first authentic TM domain is consistent with the recent demonstration of cleavage near the GPS domain in polycystin-1 (*18*). GPS domains in members of the long-N-terminal heptahelical GPCR B family (i.e., LNB-TM7 family) are found in the N-terminal extracellular portion adjacent to the first TM domain (*19*, *41*). Glycosylation reporter fusion proteins ending after the loop regions following proposed TM domains I, III, V, VII, IX, and XI were nonglycosylated, indicating an N-extracellular/C-cytosolic membrane-spanning orientation for these TM domains, while fusion proteins terminating after proposed TM domains II, IV, VI, VIII, X, and 11 resulted in either glycosylated or both glycosylated and nonglycosylated species. The simplest interpretation of these data was that the 11 TM domains predicted in the second topology model of polycystin-1 (*7*) were correct (Figure 2C).

The production of both glycosylated and nonglycosylated species of CD5-I−IV, CD5-I−X, and CD5-I−11 fusion proteins, even under conditions shown to promote processing, could be due to their requirement for additional topogenic information in order to efficiently integrate into the ER membrane. Hence, the topogenic properties of these putative TM domains and their C-terminal "partner" TM domains were tested alone and then together in tandem. In isolation, TM IV and V segments were shown to have relatively strong signal anchor type I and type II activities, respectively (Figures 3 and 4). These topogenic properties are consistent with formation of a helical hairpin loop by TM IV and TM V together. Protease protection assays which showed lack of protection of both the N- and C-termini of flag-IV−V support this interpretation. How, then, does one explain the ∼50% translocation efficiency of the CD5-I−IV glycosylation reporter construct (Figure 2)? Carbonate extraction assays demonstrated that the efficiency of membrane association and integration for TM IV was not increased by addition of TM V and associated loop sequences. Therefore, we propose that the reduced translocation efficiency of the glycosylation reporter in TM I−IV may have been due to the presence of a proline residue within the loop region immediately following TM IV (the loop is predicted to be only three residues in length, two of which are proline). The proline may have produced a kink in the polypeptide, making it difficult for the reporter to move through the translocon

apparatus and thus forcing the PRL portion to span the ER membrane for a portion of the fusion proteins. In support of this idea, in model systems, it has been shown that a single proline in an extracellular loop is sufficient to form a hairpin structure (*42*). Trapping of PRL within the membrane might be predicted to be an unstable conformation, and we have observed a marked reduction of the glycosylated form relative to the nonglycosylated form of CD5-TMI−IV when transfected cells are lysed 48 h after transfection rather than the usual 24 h (data not shown). Hence the ambiguous behavior of the CD5-I−IV glycosylation reporter construct may have been due to our unfortunate choice as to where to end the construct based on PCR primer considerations. Alternatively, TM domains IV and V may not completely cross the lipid bilayer to expose the small loop extracellularly but may instead be embedded within the membrane from the cytosolic side.

Glycosylation reporter fusion proteins CD5-I−X and CD5-I−11 were also a mixture of glycosylated and nonglycosylated species (Figure 2). When tested alone in a flag-TM-glycosylation reporter construct, TM X had relatively inefficient signal sequence activity (Figure 6). However, of the TM X fusion proteins synthesized at and integrated within the microsomal membrane, the majority had a C-lumenal orientation, suggesting that TM X does possess inherent signal anchor type II activity. Protease protection assays with both the CD5- and flag-X fusion proteins demonstrated that TM X has membrane-spanning ability (Figures 5 and 6). These data suggest that the proposed TM X is indeed a TM domain with a propensity for an N-cytosolic and C-lumenal orientation. A similar construct with proposed TM domain 11 sequences, flag-11, appeared to have some weak signal sequence or membrane-association property as illustrated by its association with microsomal membrane pellets in the Tris−sucrose buffer (Figure 6). However, these sequences were either unable to "gate" (open) the translocon or to integrate, and hence the fusion protein was extractable by carbonate buffer. The inability of TM 11 to integrate within or to span the membrane was demonstrated by its weak stop transfer activity (Figure 5). These results argue against a membrane-spanning function for proposed TM 11 but suggest that 11 may have some membrane-associated function perhaps as a portion of a pore loop (*43*) or some related vestigial structure. Similar topogenic properties have been demonstrated for the pore loop region of a couple of K^+ channels (*31*, *44*). In this respect, loop 11 has a "homologous" location with the proposed pore region of polycystin-2 (*45*, *46*), is relatively hydrophobic (Figure 1A), and has partial helix-forming propensity. The resemblance between loop 11 and a pore loop structure would be consistent with previous proposals that polycystin-1 could form or be part of an ion channel, which were based on shared homologous regions with known channel proteins (*6*, *7*). However, channel activity for polycystin-1 alone has not been demonstrated (*4*, *15*, *47*).

Unlike CD5-I−X and CD5-I−11 fusion proteins, CD5-I−XI, the longest polycystin-TM glycosylation reporter fusion protein, was not glycosylated when expressed in vivo (Figure 2), suggesting that the final membrane-spanning domain was contained within its additional sequences. This was confirmed by studies with the individual TM XI fusion constructs which showed stop transfer and membrane-spanning ability for CD5-XI (Figure 5) and strong signal sequence and signal anchor activity for flag-XI (Figure 6). Results from protease protection assays demonstrated that the N-terminal portion of the flag-XI fusion protein was intralumenal and the C-terminus was cytosolic. Therefore, the topogenic properties of the individual TM domains X, 11, and XI are consistent with formation of the final TM-extracellular loop (or pore)-TM portion of polycystin-1, respectively. Collectively, these data provide experimental evidence that polycystin-1 has 11 membrane-spanning domains that support the second polycystin-1 topology model (*7*).

Surprisingly, in the flag-X−11−XI fusion protein, TM X did not integrate within the microsomal membrane with a type II orientation, as it had in both the flag-X and flag-X−11 fusion proteins. Instead, the N-terminal portion of flag-X−11−XI was shown to be lumenal (Figure 7). A possible explanation for this apparent discrepancy may lie in the relative topogenic strength of individual TM domains X and XI. In addition, sequences not present in the flag-X−11−XI fusion protein (perhaps TM IX) may be required in order to attain the correct topology of these C-terminal TM domains. Perhaps during synthesis of (full-length) polycystin-1, once TM IX has integrated within the ER membrane, the topogenic properties of nascent TM X would not be sufficient to allow it to efficiently direct translocation of its C-terminal loop region, and therefore it would remain outside the translocon. This scenario is consistent with the relatively minor amount of CD5-I−X reporter fusion protein that was glycosylated. Once TM XI is translated, however, its relatively strong signal sequence and signal anchor type I properties could direct the membrane insertion of the preceding N-terminal TM X and loop sequences. Therefore, by the cooperation of multiple topogenic determinants, TM X would come to span the ER membrane in a signal anchor type II orientation. Similar mechanisms of membrane integration have been described for erythrocyte band 3, yeast sec61p, and CFTR proteins where TM segments with weak topogenic function were given a transmembrane orientation by their following TM domains (*27*, *29*, *40*). It was fortuitous that our experimental approach to test the proposed TM domains of polycystin-1 also yielded information on its transmembrane biogenesis. These data suggest that the biogenesis of polycystin-1 is somewhat complex and occurs via multiple integration mechanisms. The first 9 TM domains (I−IX) appear to integrate within the ER membrane by a simple, sequential mechanism. The integration of the final two TM domains, X and XI, however, may involve some type of non-cotranslational cooperative mechanism and will require additional studies.

This work is the first experimental analysis of the membrane-spanning domains of polycystin-1. Since the initial discovery of the PKD1 gene, support for an 11 TM domain structure has come from comparative hydropathy analyses of the members of the polycystin-1-related protein family [i.e., PKDREJ (*48*), suREJ3 (*49*), PKD1L1 (*50*), PKD1L2, and PKD1L3 (*51*)] and of known polycystin-1 orthologues [from mouse (*52*), dog (*53*), pufferfish (*7*), and *Caenorhabditis elegans* (*54*)], which have shown conservation of 11 hydrophobic regions. These evolutionary analyses coupled with our experimental data make a very strong case for an 11 TM domain structure for polycystin-1. It will be

interesting for future studies to determine how the transmembrane domains contribute to the various functions ascribed to polycystin-1 and what effect disease-associated mutations have on polycystin-1 membrane-associated structure and biogenesis. Notably, a number of missense mutations/polymorphisms reported in PKD1 families are located within or near various TM domains (*55*−*57*), and recently, an ENU mutagenesis-derived mouse model was generated that results in a null phenotype due to a missense mutation within TM domain I (*58*, *59*).

ACKNOWLEDGMENT

We gratefully acknowledge D. Harris for providing the glycosylation reporter tag, A. M. Frischauf and S. K. Heath for providing the mouse polycystin-1 cDNA, James Calvet for editorial comments, and Brenda Magenheimer for assistance with experiments utilizing the 293T cells. The investigators are members of the Kansas Interdisciplinary Center for PKD Research. In memory of Nancy M. Nims.

REFERENCES

1. Igarashi, P., and Somlo, S. (2002) *J. Am. Soc. Nephrol. 13*, 2384−2398.
2. European Polycystic Kidney Disease Consortium (1994) *Cell 77*, 881−894.
3. Murcia, N., Sweeney, W., Jr., and Avner, E. (1999) *Kidney Int. 55*, 1187−1197.
4. Ikeda, M., and Guggino, W. (2002) *Curr. Opin. Nephrol. Hypertens. 11*, 539−545.
5. Hughes, J., Ward, C., Peral, B., Aspinwall, R., Clark, K., San Millan, J., Gamble, V., and Harris, P. (1995) *Nat. Genet. 10*, 151−160.
6. Mochizuki, T., Wu, G., Hayashi, T., Xenophontos, S., Veldhuisen, B., Saris, J., Reynolds, D., Cai, Y., Gabpw, P., Pierides, A., Kimberling, W., Breuning, M., Deltas, C., Peters, D., and Somlo, S. (1996) *Science 272*, 1339−1342.
7. Sanford, R., Sgotto, B., Aparicio, S., Brenner, S., Vaudin, M., Wilson, R., Chissoe, S., Pepin, K., Bateman, A., Chothia, C., Hughes, J., and Harris, P. (1997) *Hum. Mol. Genet. 6*, 1483−1489.
8. Moy, G., Mendoza, L., Schulz, J., Swanson, W., Glabe, C., and Vacquier, V. (1996) *J. Cell Biol. 133*, 809−817.
9. Boletta, A., Qian, F., Onuchic, L., Bragonzi, A., Cortese, M., Deen, P., Courtoy, P., Soria, M., Devuyst, O., Monaco, L., and Germino, G. (2001) *Am. J. Kidney Dis. 38*, 1421−1429.
10. Malhas, A., Abuknesha, R., and Price, R. (2002) *J. Am. Soc. Nephrol. 13*, 19−26.
11. Ibraghimov-Beskrovnaya, O., Bukanov, N., Donohue, L., Dackowski, W., Klinger, K., and Landes, G. (2000) *Hum. Mol. Genet. 9*, 1641−1649.
12. Kim, E., Arnould, T., Sellin, L., Benzing, T., Fan, M., Gruning, W., Sokol, S., Drummond, I., and Walz, G. (1999) *J. Biol. Chem. 274*, 4947−4953.
13. Arnould, T., Kim, E., Tsiokas, L., Jochimsen, F., Gruning, W., Chang, J., and Walz, G. (1998) *J. Biol. Chem. 273*, 6013−6018.
14. Bhunia, A., Piontek, K., Boletta, A., Liu, L., Qian, F., Xu, P.-N., Germino, F., and Germino, G. (2002) *Cell 109*, 157−168.
15. Delmas, P., Nomura, H., Li, X., Lakkis, M., Luo, Y., Segal, Y., Fernandez-Fernandez, J., Harris, P., Frischauf, A.-M., Brown, D., and Zhou, J. (2002) *J. Biol. Chem. 277*, 11276−11283.
16. Parnell, S., Magenheimer, B., Maser, R., Zien, C., Frischauf, A., and Calvet, J. (2002) *J. Biol. Chem. 277*, 19566−19572.
17. Parnell, S., Magenheimer, B., Maser, R., Rankin, C., Smine, A., Okamoto, T., and Calvet, J. (1998) *Biochem. Biophys. Res. Commun. 251*, 625−631.
18. Qian, F., Boletta, A., Bhunia, A., Xu, H., Liu, L., Ahrabi, A., Watnick, T., Zhou, F., and Germino, G. (2002) *Proc. Natl. Acad. Sci. U.S.A. 99*, 16981−16986.
19. Stacey, M., Lin, H., Gordon, S., and McKnight, A. (2000) *Trends Biochem. Sci. 25*, 284−289.
20. Obermann, H., Samalecos, A., Osterhoff, C., Schroder, B., Heller, R., and Kirchhoff, C. (2003) *Mol. Reprod. Dev. 64*, 13−26.
21. Krasnoperov, V., Lu, Y., Buryanovsky, L., Neubert, T., Ichtchenko, K., and Petrenko, A. (2002) *J. Biol. Chem. 277*, 46518−46526.
22. Gether, U. (2000) *Endocr. Rev. 21*, 90−113.
23. Johnson, A., and van Waes, M. (1999) *Annu. Rev. Cell Dev. Biol. 15*, 799−842.
24. Goder, V., and Spiess, M. (2001) *FEBS Lett. 504*, 87−93.
25. Blobel, G. (1980) *Proc. Natl. Acad. Sci. U.S.A. 77*, 1496−1500.
26. Wessels, H., and Spiess, M. (1988) *Cell 55*, 61−70.
27. Ota, K., Sakaguchi, M., Hamasaki, N., and Mihara, K. (1998) *J. Biol. Chem. 273*, 28286−28291.
28. Ota, K., Sakaguchi, M., Hamasaki, N., and Mihara, K. (2000) *J. Biol. Chem. 275*, 29743−29748.
29. Lu, Y., Xiong, X., Helm, A., Kimani, K., Bragin, A., and Skach, W. R. (1998) *J. Biol. Chem. 273*, 568−576.
30. Skach, W., and Lingappa, V. (1993) *J. Biol. Chem. 268*, 235252−235261.
31. Sato, Y., Sakaguchi, M., Goshima, S., Nakamura, T., and Uozumi, N. (2002) *Proc. Natl. Acad. Sci. U.S.A. 99*, 60−65.
32. Marshall, R. (1972) *Annu. Rev. Biochem. 41*, 673−702.
33. Lehmann, S., Chiesa, R., and Harris, D. (1997) *J. Biol. Chem. 272*, 12047−12051.
34. Fujiki, Y., Hubbard, A. L., Fowler, S., and Lazarow, P. B. (1982) *J. Cell Biol. 93*, 97−102.
35. Kyte, J., and Doolittle, R. (1982) *J. Mol. Biol. 157*, 105−132.
36. Ponting, C., Hofmann, K., and Bork, P. (1999) *Curr. Biol. 9*, R585−R588.
37. Aberijon, C., and Hirschberg, C. (1992) *Trends Biochem. Sci. 17*, 32−36.
38. Rothman, R., Andrews, D., Calayag, M., and Lingappa, V. (1988) *J. Biol. Chem. 263*, 10470−10480.
39. Hartmann, E., Rapoport, T., and Lodish, H. (1989) *Proc. Natl. Acad. Sci. U.S.A. 86*, 5786−5790.
40. Wilkinson, B. M., Critchley, A. J., and Stirling, C. J. (1996) *J. Biol. Chem. 271*, 25590−25597.
41. Kierszenbaum, A. (2003) *Mol. Reprod. Dev. 64*, 1−3.
42. Nilsson, I., and von Heijne, G. (1998) *J. Mol. Biol. 284*, 1185−1189.
43. MacKinnon, R. (1995) *Neuron 14*, 889−892.
44. Tu, L. W., Wang, J., Helm, A., Skach, W. R., and Deutsch, C. (2000) *Biochemistry 39*, 824−836.
45. Nomura, H., Turco, A., Pei, Y., Kalaydjieva, L., Schiavello, T., Weremowicz, S., Ji, W., Morton, C., Meisler, M., Reeders, S., and Zhou, J. (1998) *J. Biol. Chem. 273*, 25967−25973.
46. Tsiokas, L., Arnould, T., Zhu, C., Kim, E., Walz, G., and Sukhatme, V. (1999) *Proc. Natl. Acad. Sci. U.S.A. 96*, 3934−3939.
47. Hanaoka, K., Qian, F., Boletta, A., Bhunia, A., Piontek, K., Tsiokas, L., Sukhatme, V., Guggino, W., and Germino, G. (2000) *Nature 408*, 990−994.
48. Hughes, J., Ward, C., Aspinwall, R., Butler, R., and Harris, P. (1999) *Hum. Mol. Genet. 8*, 543−549.
49. Mengerink, K., Moy, G., and Vacquier, V. (2002) *J. Biol. Chem. 277*, 943−948.
50. Yuasa, T., Venugopal, B., Weremowicz, S., Morton, C., Guo, L., and Zhou, J. (2002) *Genomics 79*, 376−386.
51. Li, A., Tian, X., Sung, S., and Somlo, S. (2003) *Genomics 81*, 596−608.
52. Lohning, C., Nowicka, U., and Frischauf, A.-M. (1997) *Mamm. Genome 8*, 307−311.
53. Dackowski, W., Luderer, H., Manavalan, P., Bukanov, N., Russo, R., Roberts, B., Klinger, K., and Ibraghimov-Beskrovnaya, O. (2002) *Genomics 80*, 105−112.
54. Barr, M., and Sternberg, P. (1999) *Nature 401*, 386−389.
55. Eo, H.-S., Lee, J., Ahn, C., Cho, J., Hwang, D., Hwang, Y., Lee, E., Kim, Y., Han, J., Kim, S., Lee, J., Jeong, D., Lee, S., and Kim, U. (2002) *Clin. Genet. 62*, 169−174.
56. Daniells, C., Maheshwar, M., Lazarou, L., Davies, F., Coles, G., and Ravine, D. (1998) *Hum. Genet. 102*, 216−220.
57. Turco, A., Rossetti, S., Bresin, E., Englisch, S., Corra, S., and Pignatti, P. (1997) *Hum. Mutat. 10*, 164−167.
58. Lu, W., Herron, B., Arnaout, M., and Beier, D. (2002) *J. Am. Soc. Nephrol. 13*, 113A.
59. Herron, B., Lu, W., Rao, C., Liu, S., Peters, H., Bronson, R., Justice, M., McDonald, D., and Beier, D. (2002) *Nat. Genet. 30*, 185−189.

BI035074C